Published in: Journal of Nuclear Materials 494 (2017) 211

The high-flux effect on deuterium retention in TiC and TaC doped tungsten at high temperatures

Mikhail Zibrov[a,b,c,d,e], Kirill Bystrov[b], Matej Mayer[a], Thomas W. Morgan[b], Hiroaki Kurishita[f]

[a]*Max-Planck-Institut für Plasmaphysik, Boltzmannstraße 2, D-85748 Garching, Germany*

[b]*DIFFER – Dutch Institute for Fundamental Energy Research, De Zaale 20, 5612 AJ Eindhoven, The Netherlands*

[c]*Department of Applied Physics, Ghent University, Sint-Pietersnieuwstraat 41, B-9000 Ghent, Belgium*

[d]*Physik-Department E28, Technische Universität München, James-Franck-Straße 1, D-85748 Garching, Germany*

[e]*National Research Nuclear University MEPhI (Moscow Engineering Physics Institute), Kashirskoe shosse 31, 115409 Moscow, Russia*

[f]*International Research Centre for Nuclear Materials Science, IMR, Tohoku University, Oarai, Ibaraki 311-1313, Japan*

E-mail: Mikhail.Zibrov@ipp.mpg.de

Abstract

Samples made of tungsten (W) doped either with titanium carbide (W-1.1TiC) or tantalum carbide (W-3.3TaC) were exposed to a low-energy (40 eV/D), high-flux ($1.8\text{-}5\times10^{23}$ D/m^{2}s) deuterium (D) plasma at temperatures of about 800 K, 1050 K, and 1250 K to a fluence of about 1×10^{27} D/m^2. The deuterium (D) inventory in the samples was examined by nuclear reaction analysis and thermal desorption spectroscopy. At 800 K the D bulk concentrations and total D inventories in W-1.1TiC and W-3.3TaC were more than one order of magnitude higher compared to that in pure polycrystalline W. At 1050 K and 1250 K the D concentrations in all types of samples were very low ($\leq10^{-5}$ at. fr.); however the D inventories in W-1.1TiC were significantly higher compared to those in W-3.3TaC and pure W. It is suggested that D trapping inside the carbide precipitates and at their boundaries is essential at high temperatures and high incident fluxes, especially in W-1.1TiC.

Keywords: Tungsten, Deuterium retention, Surface modifications, Blistering, Thermal desorption

1. Introduction

Tungsten (W) will be used as a plasma-facing material (PFM) in the divertor region in ITER, and its use in future fusion devices is also very likely [1, 2]. The use of W as a PFM is attractive due to its high melting temperature, high sputtering threshold, high thermal conductivity, and relatively low long-term activation after neutron irradiation. At the same time, one of the critical problems of W is related to its poor thermo-mechanical properties, such as high ductile-to-brittle transition temperature, rather poor thermal shock resistance, and embrittlement after recrystallization and irradiation (by neutrons and ions) [1]. Therefore presently many efforts are spent on development of advanced W–based materials with improved thermo-mechanical properties. Among these toughened, fine-grained, recrystallized (TFGR) W-based materials doped either with titanium carbide (TiC) or tantalum carbide (TaC) developed at Tohoku University (Japan) are quite promising because of their improved ductility at low temperatures, enhanced resistance against radiation-induced embrittlement, and improved thermal shock resistance [3, 4]. However, it was shown that deuterium (D) accumulation in these materials is higher compared to that in pure polycrystalline W at temperatures above 573 K [5-9]. In particular, the previous experimental results suggested that D trapping inside the carbide precipitates can be essential at high temperatures (≥ 800 K), especially in TiC doped W [9]. It was proposed that at high temperatures the concentration of D trapped in the carbide precipitates should increase with increasing concentration of solute D during the plasma exposure (i.e. with incident ion flux). Consequently, relatively high concentrations of retained D in doped W materials might be expected under a high-flux plasma exposure at high temperatures.

In ITER and next-step fusion devices the divertor plates will be subjected to high fluxes (up to 10^{24} ions/m^2s) of low-energy (several tens of eV) hydrogen isotopes. The stationary surface temperature will strongly vary along the divertor target in ITER (in the range of 450-1400 K), and can reach even higher values during transient events like Edge Localized Modes (ELMs) and disruptions [2]. Thus, it is essential to investigate experimentally the trapping effects in doped W materials under divertor-relevant particle fluxes and in a wide range of temperatures.

2. Experimental details

2.1. Sample preparation

Samples made of TFGR W doped either with 1.1 wt.% (3.3 at.%) TiC (W-1.1TiC) or with 3.3 wt.% (3.2 at.%) TaC (W-3.3TaC) with dimensions of $10\times10\times1.2$ mm^3 manufactured at Tohoku University (Japan) were used. The sample fabrication procedure consisted of several steps: (1) mechanical alloying of W and TiC (or TaC) powders in H_2 atmosphere; (2) degassing of the alloyed powder; (3) encapsulation of the powder in a steel capsule in vacuum; (4) hot isostatic pressing at 1623 K; (5) grain boundary sliding-based microstructural modification (GSMM) - a deformation process at 1923 K in vacuum. The materials were composed of isotropic W grains with dimensions in the range of 0.5-5 μm and carbide precipitates with dimensions in the range of 0.05-1 μm, which were located both inside the W grains and at the grain boundaries [7]. Further details about the manufacturing of the samples as well as about their microstructure can be found elsewhere [3, 4]. In addition, samples made of hot-rolled pure polycrystalline W with dimensions of $10\times10\times0.8$ mm^3 and purity of 99.97 wt.% manufactured by PLANSEE (Austria) were used as a reference material. Those samples had flattened grains elongated parallel to the surface with a length up to a few μm and a thickness up to 1 μm (perpendicular to the surface) [10]. All the samples were polished to a mirror-like finish and then annealed in vacuum at 1173 K for 2 hours to remove residual hydrogen and relieve stresses.

2.2. Deuterium plasma exposure

The samples were exposed to a pure D plasma in the linear plasma generator Pilot-PSI (DIFFER, The Netherlands) [11, 12]. The base pressure in the vacuum chamber was about 10^{-1} Pa and increased to about 1 Pa during the plasma operation. The plasma consisting of predominantly D^+ ions was generated by a DC cascaded arc source and transported to the target by applying a constant axial magnetic field of 0.2 T allowing performing steady-state plasma exposures. The radial profiles of electron temperature and density of the plasma beam were measured by Thomson scattering at a distance of about 2 cm from the target. The incident ion flux calculated using the Bohm criterion had a Gaussian radial distribution with a full width at half maximum (FWHM) in the range of 15-20 mm. The maximum ion flux in the beam centre varied in the range of $1.8\text{-}5\times10^{23}$ D/m^{2}s in different experiments, but did not change significantly

within the duration of each experiment. The difference between the flux in the beam centre and the averaged one over the entire exposed area of the specimen was within 20%.

The target was clamped to a water-cooled copper holder with a Grafoil® flexible graphite interlayer by using a clamping ring made of TZM alloy. A bias voltage of -40 V was applied to the target holder during exposures resulting in a mean incident ion energy close to 40 eV. The surface temperature of the sample during the plasma exposure was governed by the balance between the heat flux on the target carried by the plasma beam and cooling by thermal conduction. Adjustment of the temperature was obtained mainly by varying the physical contact of the sample with the holder – by making a hole in the graphite interlayer underneath the exposed area and by varying the tightening torque of the clamping ring. Fine adjustment of the temperature was achieved by varying the incident ion flux during the beginning of the exposure ($\leq$ 100 s).

The surface temperature in the sample centre during the plasma exposure was monitored by a multi-wavelength infrared (IR) pyrometer (FAR associates FMPI). The pyrometer measured the thermal emission spectrum from the surface area (diameter about 1 mm) in the wavelength range of 0.9–1.7 μm and fitted it to Planck's radiation law in real-time in order to yield the surface temperature. This allowed an accurate temperature determination without prior knowledge of the material spectral emissivity even for non-grey sources, i.e. when emissivity depends on the wavelength, which is the case for W [13]. The accuracy of the temperature measurement reported by the pyrometer was always within 7 K. The lateral distribution of the surface temperature of the target during the plasma exposure was determined by IR thermography using a fast camera (FLIR SC7500-MB) measuring in the mid-wave IR range of 3.5–5 μm. The results of the IR thermography are dependent on the knowledge of the spectral emissivity of the surface, which depends strongly on the surface finish and also on the surface temperature itself. The emissivity of W-1.1TiC and W-3.3TaC is unknown and can differ from that of pure W. Therefore during processing of the raw IR data the emissivity of each sample was adjusted in a way that the surface temperature in the sample centre matched that measured by the pyrometer. The surface temperature distributions were then obtained under the following assumptions: 1. all area of interest had the same known background temperature; 2. the IR background signal did not change during the measurement; 3. the emissivity is independent of the surface temperature.

The plasma exposures were carried out at temperatures in the centres of the samples of about 800 K, 1050 K, and 1250 K. The temporal evolution of the temperatures in the centres of all the specimens measured by the pyrometer is plotted in **Fig. 1**. The final surface temperatures were reached practically within 100 s after the beginning of the plasma exposure; the cooling of the targets to room temperature after the end of the exposures typically occurred within 30 s. The scatter of the time-averaged surface temperature in the sample centre among different targets was within 40 K. The difference between the temperatures at the beginning and at the end of the exposures was within 75 K, which was caused by reduction of the incident ion flux due to a decrease of the B-field strength (due to warming-up of the B-field coils). **Fig. 2** shows the lateral temperature distributions for all the specimens measured by IR thermography 5 min after the beginning of the plasma exposure, i.e. when the temperatures had already stabilized. Please note that the strong temperature decrease observed very close to the edges of the targets is likely artificial and caused by looking at the clamping ring. As it can be seen, the measured distributions are not symmetric with respect to the sample centre. This can be caused by several reasons. Firstly, since the thermal contact between the sample and the holder was deliberately reduced, this could result in its asymmetry. Secondly, since the targets were mirror-polished and had a low emissivity, i.e. high reflectivity, thermal radiation from hot components in the vacuum vessel reflected by the target could be laterally non-uniform, thus, artificially increasing the deduced surface temperature of some parts of the specimen. Finally, the centre of the beam could also not exactly match the centre of the sample. Unfortunately, it is not possible to determine the contribution of each factor. Thus, the lateral variation of the surface temperature across the specimen surface of about 200 K should be considered as an upper limit. Although W-1.1TiC has up to 35% lower thermal conductivity (in the investigated temperature range) compared to pure W [14], the differences between temperature distributions among different types of samples are mainly caused by the non-reproducible clamping. Due to the small thicknesses of the samples the characteristic length scales of temperature variation in the depth are much larger than the maximum penetration depth of D in the present experiments. Thus, temperature non-homogeneities in depth have a negligible influence on the results of the experiments.

The incident ion fluence was close to 1×10^{27} D/m^2 in all experiments. Since all the plasma exposures were carried out in a steady-state regime for at least 30 min, the ramping up and down

of the surface temperature at the beginning and at the end of the exposure, respectively, has a negligible influence on the interpretation of the results.

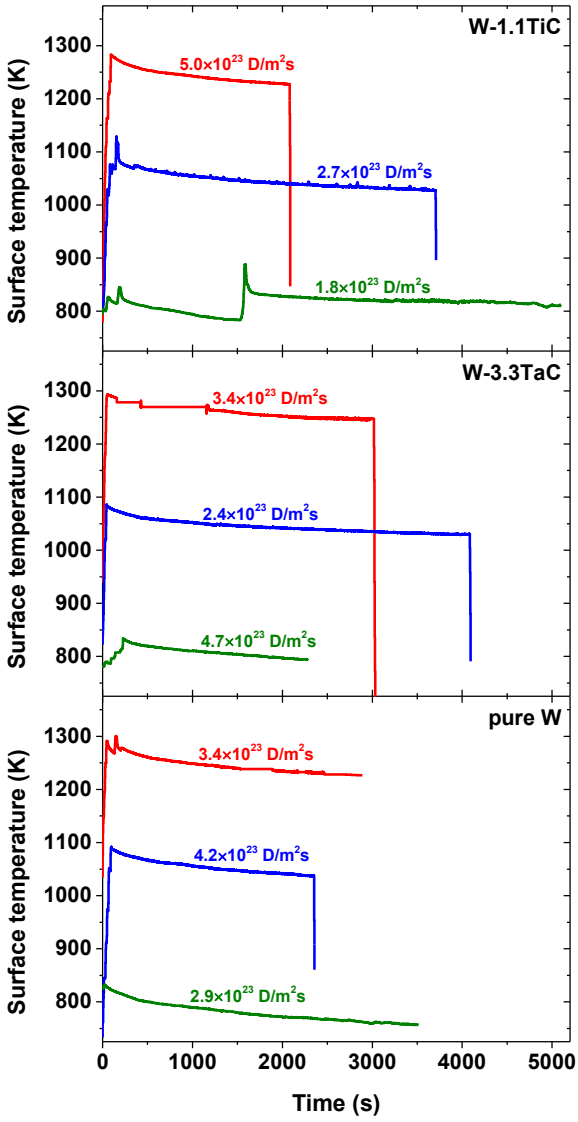

Fig. 1. Temporal evolutions of the surface temperature in the sample centre during the high-flux D plasma exposure for W-1.1TiC, W-3.3TaC, and pure polycrystalline W. The temperatures were determined by pyrometry. The average incident ion flux during the corresponding exposure is indicated above each curve. Note that the exposure times were different in order to achieve the same fluence of about 1×10^{27} D/m^2 for each sample. Also note that the pyrometer was not able to measure temperatures below 700 K.

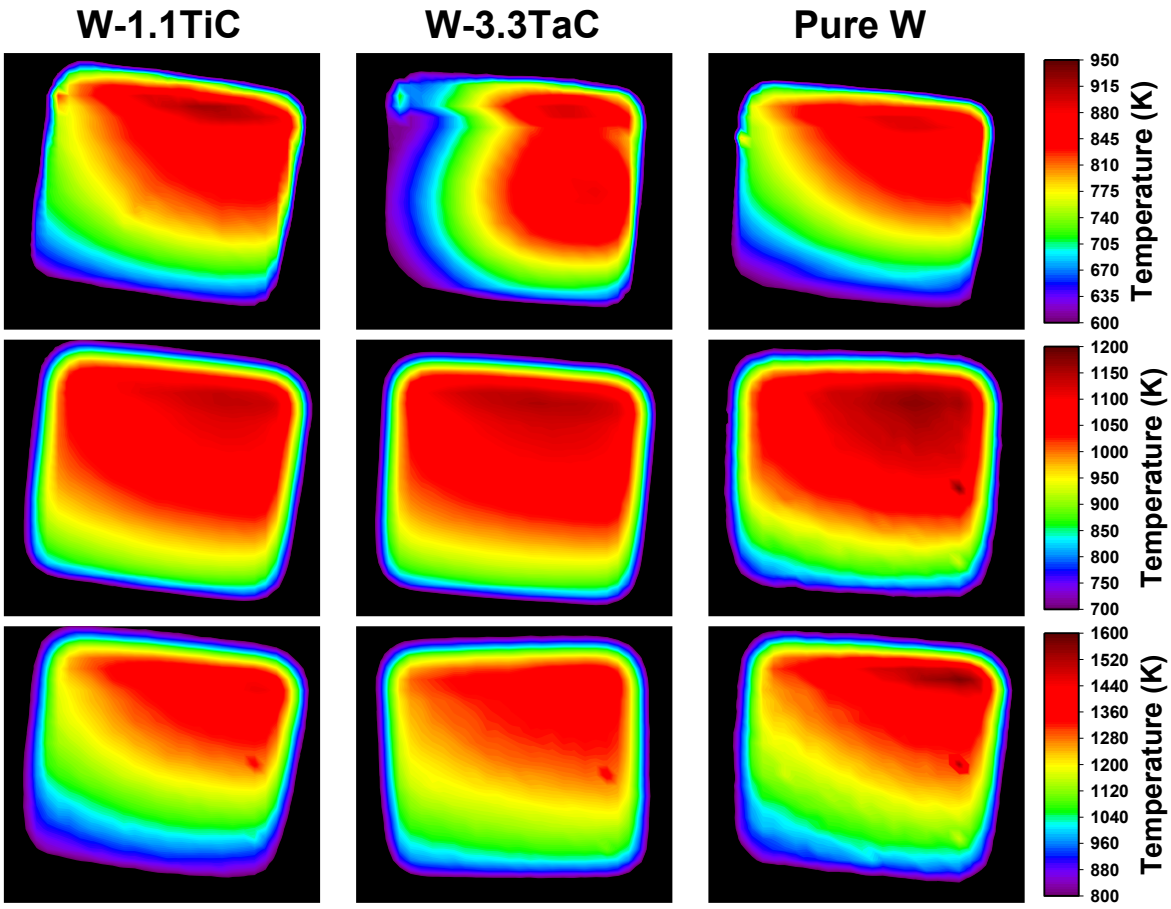

Fig. 2. Lateral temperature distributions of W-1.1TiC (left column), W-3.3TaC (centre), and pure polycrystalline W (right column) after 5 min of the high-flux D plasma exposure derived from the IR thermography. The same temperature scale bar is valid for the whole row. Note that the strong temperature decrease observed very close to the edges of the targets is likely artificial and caused by looking at the clamping ring.

2.3. Sample analyses

D depth distributions in the samples up to a depth of 7 μm were measured using D(^{3}He,p)α nuclear reaction analysis (NRA) at the 3 MV tandem accelerator (IPP, Garching) about six months after the plasma exposures. Eight different ^{3}He energies varying from 0.5 MeV to 4.5 MeV were used in order to obtain information from different sample depths [15]. Energy spectra of both protons and α particles were transformed into D concentration profiles using the NRADC programme [16] together with SIMNRA [17]. The accumulated charge of ^{3}He ions for

each sample at each energy was in the range of 30–50 μC, resulting in the minimal detectable D concentration of a few times 10^{-6} atomic fractions (at. fr.).

Thermal desorption spectra (TDS) were measured in the TESS installation (IPP, Garching) [18] about eighteen months after the plasma exposures. The samples were placed in a quartz tube and heated by radiation from an external furnace up to a temperature of 1280 K at a background pressure below 10^{-6} Pa. The furnace was linearly heated with a rate of 0.25 K/s. The real sample temperature versus the measured oven temperature was calibrated in an independent experiment by a thermocouple spot-welded to the sample. At the beginning of the temperature ramp the heating rate was nonlinear up to 800 K (see **Fig. 4**). The release of 12 masses was monitored by a quadrupole mass spectrometer (QMS). In order to determine the total amount of retained D, the QMS signal for mass 4 (D_2) was calibrated using a calibrated leak. The relative QMS sensitivities for masses 3 (HD) and 4 were determined by using the procedures described in [19]. The total D inventory was then calculated as the sum of the D_2 and HD contributions. In order to roughly estimate the contribution of heavy water, the relative QMS sensitivities of D_2O to D_2 and of HDO to HD were assumed to be the same as that of H_2O to H_2, which was taken from [20].

The surface morphology of the samples after the plasma exposures was investigated in a scanning electron microscope (SEM) FEI HELIOS NanoLab 600 (IPP, Garching). Examination of all the exposed specimens did not indicate the presence of any apparent deposited impurity layers or particles. In addition, the analysis of the surface area of W-1.1TiC and W-3.3TaC samples exposed at about 800 K by energy-dispersive X-ray spectroscopy (EDX) with 15 keV incident electrons revealed the presence of only oxygen and carbon impurities, and the EDX spectra of the plasma-exposed and unexposed samples were almost identical. Furthermore, the analysis of all the plasma-exposed pure W samples (which intrinsically have a low amount of carbon) using the $^{12}C(^3He,p_{0,1,2})^{14}N$ nuclear reactions with 4.5 MeV ^3He ions demonstrated that the amount of carbon on the surface was close to 10^{20} C/m^2, i.e. very similar to that on W samples that were not exposed to plasma. Thus, it can be concluded that a few nm thick carbon- and oxygen-containing layers were present on the targets due to their exposure to air.

After the TDS analyses four samples were additionally investigated with X-ray photoelectron spectroscopy (XPS) in a PHI 5600 ESCA system using a non-monochromatic Al K_α X-ray source. Apart from the carbon and oxygen impurities, the presence of silicon on the surfaces was also detected, but its concentration was moderate (< 10%) and it cannot be excluded

that the silicon contamination was introduced during the TDS measurements (since the samples were heated in a quartz tube). Overall, the amount of impurities on the exposed surfaces was quite small, thus, their presence should have little influence on the measured D retention.

The samples were always stored in between different analyses in a vacuum desiccator since the prolonged contact of the exposed samples with air can result in large fractions of D released as heavy water during TDS measurements, which complicates the interpretation of the experimental results [21].

3. Results

Fig. 3 shows the measured D depth distributions in W-1.1TiC and W-3.3TaC exposed at about 800 K. The measurements were carried out in the centres of the samples (the diameter of the analysing beam was about 1 mm), where the local surface temperature was close to 800 K as determined by the pyrometer (the diameter of the collecting area was also around 1 mm). For comparison the results of the previous low-flux (10^{20} D/m^{2}s) plasma exposures and D_2 gas (100 kPa) exposures of the same type of samples at a similar temperature [9] are also shown. The D depth profiles in W-1.1TiC and W-3.3TaC exposed to a high-flux plasma both exhibited a constant D bulk concentration within the analysis range (≤ 7 μm), except for the enhanced D concentration in the sub-surface layer (≤ 1 μm). In W-1.1TiC the D bulk concentration after the high-flux plasma exposure was more than an order of magnitude higher compared to that after the low-flux plasma exposure, and was also about two times higher compared to that after the exposure to D_2 gas. In W-3.3TaC the D bulk concentration after the high-flux plasma exposure was more than an order of magnitude higher compared to those both after the low-flux plasma exposure and the D_2 gas exposure (not shown). In pure polycrystalline W exposed at the same temperature the D concentration was considerable only in a shallow sub-surface layer (≤ 1 μm); the D concentration at larger depths was low ($\leq 10^{-5}$ at. fr.) and was not measured in the present experiments.

In W-3.3TaC and pure polycrystalline W samples exposed at higher temperatures (about 1050 K and 1250 K) the D concentrations were below the sensitivity limit of NRA. In the W-1.1TiC samples exposed at these temperatures the D bulk concentrations were low ($\leq 10^{-5}$ at. fr.),

although definitely higher compared to those in W-3.3TaC and pure polycrystalline W, and were not measured in the present experiments.

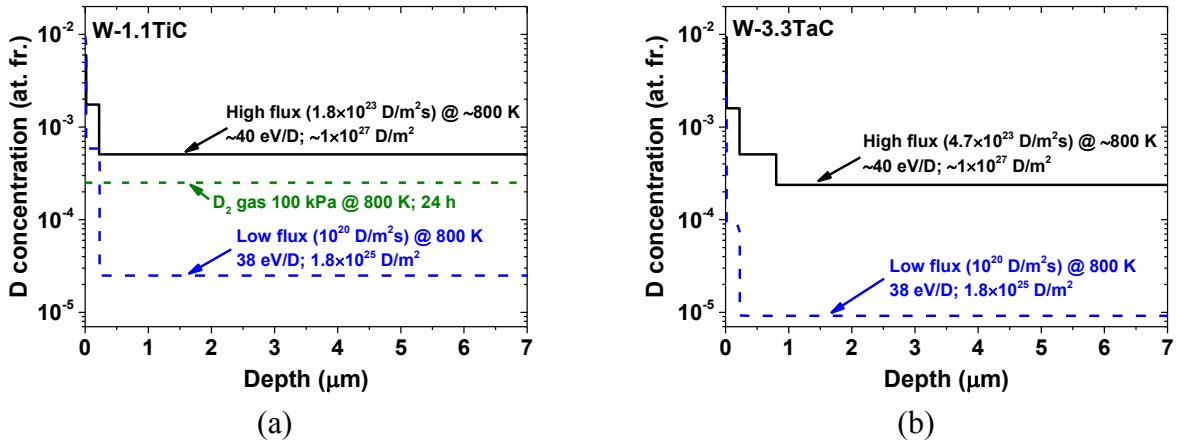

Fig. 3. Comparison of D concentration profiles in W-1.1TiC (a) and W-3.3TaC (b) exposed to a high-flux (1.8-4.7×10^{23} D/m^2s) and a low-flux (10^{20} D/m^2s) D plasma and to D_2 gas (100 kPa, 24 hours) at a temperature of about 800 K. The mean incident ion energy was near 40 eV/D and the incident fluences were around 1×10^{27} D/m^2 (high-flux exposure) and 1.8×10^{25} D/m^2 (low-flux exposure). For the samples exposed to the high-flux plasma the measurements were carried out in the sample centres, where the local surface temperature was about 800 K. The results of the low-flux plasma and D_2 gas exposures were taken from Ref. [9].

The non-uniformity of the D retention in the lateral direction, which could arise due to the temperature variation across the specimen surface and non-homogeneity of the incident ion flux, was checked by measuring with 4.5 MeV ^{3}He ions at three different spots (centre and ±2 mm). In all samples exposed near 800 K the lateral distribution of trapped D was asymmetric with respect to the sample centre, pointing to the asymmetric lateral temperature distribution derived from IR thermography (see **Fig. 2**). Although in W-1.1TiC and pure polycrystalline W the variation was moderate (up to 1.3 times in W-1.1TiC and up to 1.5 times in pure W), in W-3.3TaC it was up to 8 times and could be due to a different lateral temperature distribution during the exposure in W-3.3TaC compared to those in W-1.1TiC and pure W (**Fig. 2**). In the case of the samples exposed at higher temperatures the counting statistics of NRA was not sufficient to assess the lateral variations of D retention.

The TDS spectra after the exposures at about 800 K are presented in **Fig. 4 a**. The spectrum from W-1.1TiC had a major release peak near 960 K and a shoulder near 1200 K, and had similar peak positions as spectra both after low-flux and D_2 gas exposures reported in Ref. [9]. Pure W showed a major release peak near 940 K and a small additional peak near 700 K, also similarly to the low-flux exposure case. At the same time, the spectrum of W-3.3TaC exhibited a peak near 830 K and a shoulder near 1000 K, whereas both after low-flux and D_2 gas exposures TDS spectra exhibited a major peak near 1000 K. This can be a consequence of a strongly non-homogeneous lateral distribution of trapped D in W-3.3TaC compared to W-1.1TiC, i.e. the regions with the highest retention could had lower surface temperature during the exposure, thus, trapping sites with lower binding energies could still hold D.

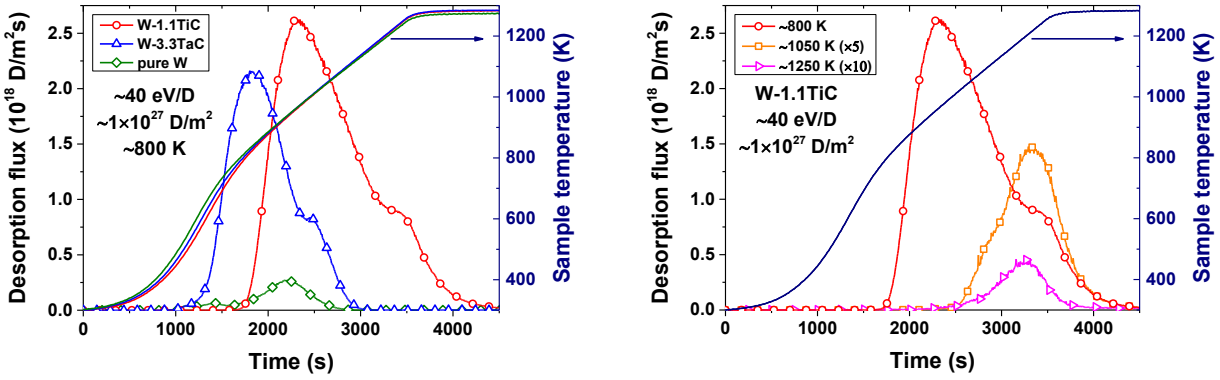

Fig. 4. Thermal desorption spectra of D_2 molecules from (a) W-1.1TiC, W-3.3TaC, and pure polycrystalline W exposed at a temperature of about 800 K, and (b) from W-1.1TiC exposed at temperatures of about 800 K, 1050 K, and 1250 K. All the samples were exposed to a high-flux D plasma to a fluence of about 1×10^{27} D/m^2. The exposure temperatures are valid for the sample centre. The evolution of the sample temperature during TDS is shown in (a) for each sample and has the same colour as the TDS spectrum of the respective sample. Note that the spectra in (b) after the exposures at about 1050 K and 1250 K are enlarged by factors of 5 and 10, respectively.

The total D inventory after the exposure at about 800 K in W-1.1TiC was about 1.6 times higher compared to that in W-3.3TaC (**Fig. 5**). The D retention in pure W was an order of magnitude lower compared to that in doped W materials under the same exposure conditions. The D retention measured by TDS was more than one order of magnitude higher compared to that

measured by NRA both in W-1.1TiC and W-3.3TaC, which can be due to the deep D diffusion beyond the analysis range of NRA. However, the laterally non-uniform distributions of trapped D (especially in W-3.3TaC) could also contribute to this difference.

The spectra for the W-1.1TiC samples exposed at about 1050 K and 1250 K both exhibited only a peak near 1200 K (**Fig. 4 b)**, and the total D inventory strongly decreased with increasing exposure temperature (**Fig. 5**). In the case of W-3.3TaC and pure polycrystalline W exposed at about 1050 K and 1250 K practically no D was released as D_2 and HD molecules; only D release in the form of heavy water (mainly HDO) was detected. Since in the present experiments it was not possible to perform absolute calibration of HDO and D_2O desorption fluxes, their contribution was roughly estimated by using the relative QMS sensitivity factors reported in [20], which yielded a very low (< 10^{19} D/m^2) D inventory in the samples.

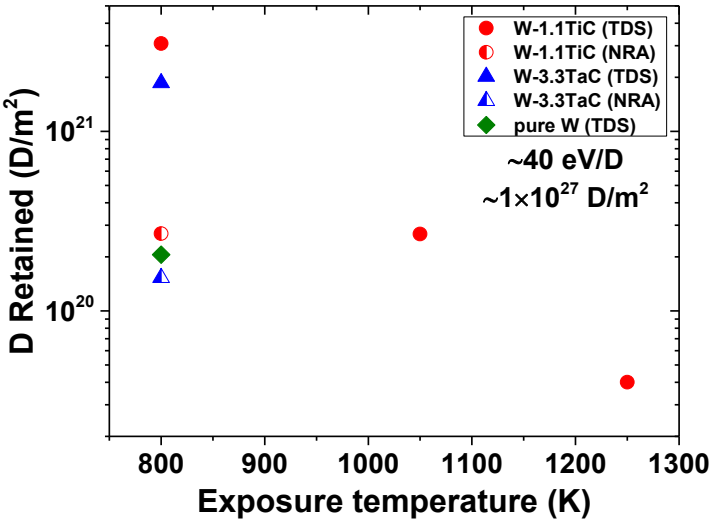

Fig. 5. D retention in W-1.1TiC, W-3.3TaC, and pure polycrystalline W exposed to a high-flux D plasma at temperatures of about 800 K, 1050 K, and 1250 K to a fluence of about 1×10^{27} D/m^2 determined by NRA and TDS. The D inventories in W-3.3TaC and pure polycrystalline W exposed at about 1050 K and 1250 K were very low (< 10^{19} D/m^2) and could not be accurately measured. Note that the exposure temperatures are valid for the sample centre.

All the samples exposed at about 800 K exhibited the formation of stepped flat-topped and irregularly-shaped structures with sharp edges and dimensions ranging from 100 nm to several

μm (**Fig. 6**). Such structures are typically referred in the literature as "protrusions" [22-24]. In addition, pure W samples demonstrated the presence of dome-shaped blister-like structures with approximately elliptic outlines and diameters up to 20 μm, which are typically referred as "blisters" [22-24].

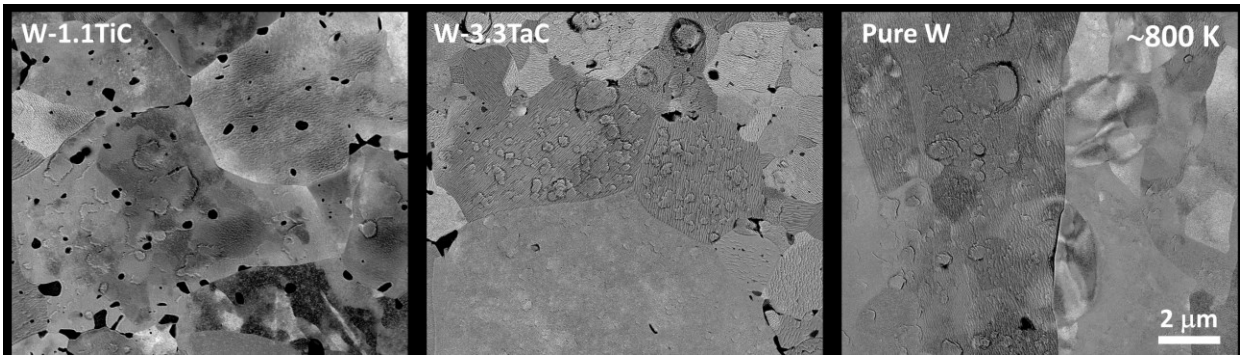

Fig. 6. SEM images of W-1.1TiC, W-3.3TaC, and pure polycrystalline W exposed to a high-flux D plasma at a temperature of about 800 K to a fluence of about 1×10^{27} D/m^2. The images were taken with backscattered electrons in the centres of the samples. The dark regions in the images of W-1.1TiC and W-3.3TaC correspond to the carbide precipitates.

On W-1.1TiC and W-3.3TaC exposed at about 1050 K no blisters and protrusions were found, whereas pure W still demonstrated the presence of blisters and protrusions. Both doped and pure W did not exhibit the presence of blisters and protrusions after the exposure at about 1250 K. Furthermore, surface roughening on the length scale ranging from several tens of nm to several hundreds of nm was observed on all the samples, similarly to previously reported cases [23, 24].

4. Discussion

The fact that at elevated temperatures the concentrations of trapped D in W-1.1TiC and W-3.3TaC were considerably higher compared to those in pure W indicates a much higher concentration of trapping sites with high binding energies in W-1.1TiC and W-3.3TaC compared to that in pure W. The carbide precipitates can serve as such high-energy trapping sites. Indeed, density functional theory (DFT) calculations of the H interaction with TiC precipitates in Fe

indicated that H isotopes can be trapped both inside the precipitates and at their boundaries [25]. At moderate temperatures H can be trapped only at the carbide boundaries due to the high activation barrier for H entering the precipitates and low H diffusivity in TiC. At high temperatures, however, H is able to enter the precipitates, diffuse into their bulk and be trapped there in lattice defects. Transition-metal carbides are known to be non-stoichiometric and to contain vacant sites in the carbon sublattice, which concentration can reach up to 50% [26]. Such carbon-vacancies can effectively trap H isotopes. For instance, DFT calculations predict a H binding energy with carbon-vacancies in TiC of 2.12 eV [27], which is higher than experimentally determined D binding energies with vacancies and vacancy clusters in W [28, 29]. Thus, in W-1.1TiC and W-3.3TaC carbide precipitates can potentially provide a large number of trapping sites, since the concentration of carbides in W-1.1TiC and W-3.3TaC is about 3 at.%.

According to the diffusion-trapping theory of H retention in metals, at high temperatures the equilibrium fractional occupancy of a particular trapping site is a result of the competition between H trapping and detrapping processes. Consequently, at a given temperature it increases with increasing H binding energy to the trapping site and the local concentration of solute H [30-32]. During plasma exposure the local steady-state concentration of solute H is proportional to the non-reflected part of the incident ion flux, if the H release is not surface-limited. Thus, at a given temperature and incident ion energy, a higher incident ion flux leads to a higher equilibrium fractional occupancy of trapping sites [32]. In the present experiments the incident ion flux was more than three orders of magnitude higher compared to that in our previous low-flux experiments [9], while the sample temperature (about 800 K) and the incident ion energy (near 40 eV/D) were close. This can explain the much higher concentrations of trapped D in W-1.1TiC and W-3.3TaC after the high-flux plasma exposures at about 800 K compared to those after the low-flux plasma exposures at a similar temperature (see **Fig. 3**). It is worth to mention that in the previous low-flux and D_2 gas exposure experiments the D retention in W-3.3TaC was similar to that in pure W at 800 K, whereas a significant difference was observed in the present high-flux experiments. Despite the two orders of magnitude difference in incident fluences (1×10^{27} D/m^2 vs. 1.8×10^{25} D/m^2 after high- and low-flux exposures, respectively), and, correspondingly, the exposure times, the above mentioned physical picture of a steady-state H concentration at a certain depth in the material is valid as long as the diffusion front of solute H has moved beyond this depth. Since the measured D depth distributions both after high- and low-

flux exposures are flat at depths beyond 1 μm, it can be concluded that in both cases the diffusion front of solute H has propagated beyond the maximum depth accessible by NRA (7 μm). Thus, the comparison of measured D concentrations after low- and high-flux exposure cases based on the above mentioned formalism is justified.

Under the high-flux exposure D was trapped in W-1.1TiC even at higher exposure temperatures (about 1050 K and 1250 K), while in W-3.3TaC (like in pure W) the retention was negligible. TDS spectra after the exposures at about 800 K show that W-1.1TiC had a high-temperature shoulder near 1200 K, while W-3.3TaC had a shoulder only near 1000 K, which indicates that W-1.1TiC has trapping sites with considerably higher binding energy compared to those in W-3.3TaC. Such differences may be related to the differences between the properties of the carbide precipitates in the materials, i.e. non-stoichiometry, activation energies for entering the precipitates, and binding energies with the defects inside the precipitates, as well as at their boundaries. Although the H isotope retention in TiC was studied extensively both experimentally [33-36] and by DFT calculations [25, 27], no data on H isotope behaviour is available for TaC.

The fact that blistering took place on both pure and doped W after the high-flux plasma exposure at about 800 K, while it was not observed after the low-flux exposure at the same temperature [9], is not surprising since in W the threshold temperature for the disappearance of blistering typically increases with increasing ion flux [37]. The absence of blistering on W-1.1TiC and W-3.3TaC exposed at about 1050 K, in contrast to pure W, can be attributed to the grain boundary strengthening provided by the presence of carbide precipitates [3, 4]. Despite the formation of protrusions on W-1.1TiC and W-3.3TaC after the exposure at about 800 K, the trapping sites introduced during their creation seem to have only a minor influence on D retention, since in pure W blistering was observed as well, but the D was detectable only in a sub-surface layer ($\leq$ 1 μm) and the total D inventory in W was much lower compared to that in W-1.1TiC and W-3.3TaC exposed under similar conditions. Consequently, it can be suggested that at such high temperatures intrinsic trapping sites in the bulk determine the total trapped inventory.

5. Conclusions

D retention in toughened, fine-grained, and recrystallized W doped either with 1.1 wt.% TiC or with 3.3 wt.% TaC has been investigated after the exposure to a high-flux D plasma at high temperatures (800-1250 K) which are expected in the ITER divertor for the inter-ELM phases of discharges. After the exposure at about 800 K the D bulk concentrations and total D inventories in W-1.1TiC and W-3.3TaC were more than one order of magnitude higher compared to that in pure polycrystalline W. Furthermore, the D bulk concentrations in W-1.1TiC and W-3.3TaC after the high-flux plasma exposure were more than one order of magnitude higher compared to those after the low-flux plasma exposures of the same materials at a similar temperature. At about 1050 K and 1250 K the D concentrations in all samples were low ($\leq 10^{-5}$ at. fr.), whereas the D inventories in W-1.1TiC were significantly higher compared to those in W-3.3TaC and pure polycrystalline W. It was concluded that the concentration of trapping sites with a high binding energy in W-1.1TiC and W-3.3TaC was much higher compared to that in pure W. Thermal desorption spectra from these materials indicated that the trapping sites in W-1.1TiC had a higher binding energy compared to those in W-3.3TaC, resulting in the wider temperature range where D retention in W-1.1TiC is significant. It is suggested that D trapping at the boundaries of the precipitates and in vacancies in the bulk of the precipitates in W-1.1TiC and W-3.3TaC becomes essential at high temperatures. The difference in D retention in W-1.1TiC and W-3.3TaC may be attributed to differences in sizes and amounts of the precipitates, their stoichiometry, activation energies for entering the precipitates, binding energies with the defects, and D diffusivity in them. The difference between D accumulation in W-1.1TiC and W-3.3TaC after low- and high-flux plasma exposures may be due to the difference in D solute concentrations in the two cases, which determines the equilibrium fractional occupancy of trapping sites inside the precipitates and at their boundaries.

Overall, from the previously reported [5-9] and the present results it can be concluded that W-1.1TiC exhibits higher D retention than pure polycrystalline W in a wide range of investigated temperatures (573-1250 K), whereas W-3.3TaC has higher retention than pure W in a more narrow temperature range (573-800 K). Although it appears that their use in fusion devices is unfavourable from the point of view of H isotope retention, one should keep in mind that in ITER and next-step fusion devices 14 MeV neutrons will create radiation defects through the whole

bulk of W plasma-facing components with a saturation concentration of about 1 at.% [32]. Thus, D retention in radiation defects can easily prevail that in the intrinsic bulk defects. However, W-1.1TiC and W-3.3TaC provide a high density of sinks (grain boundaries and carbide precipitates) for radiation defects [3, 4]. Consequently, the synergy of the presence of radiation damage and high-flux plasma exposure at high temperatures needs to be clarified for W-1.1TiC and W-3.3TaC and compared with that for pure W in order to make a definite conclusion about the possible use of such materials in fusion reactors with respect to H isotope retention.

Acknowledgements

We are grateful to T. Höschen for the XPS analysis of the samples, G. Matern and S. Elgeti for the sample preparation and SEM/EDX investigations, T. Dürbeck for the help with performing the TDS measurements, J. Dorner and M. Fußeder for the technical assistance during the ion beam analysis. This work was supported by the European Commission and carried out within the framework of the Erasmus Mundus International Doctoral College in Fusion Science and Engineering (FUSION-DC). This work has also been carried out within the framework of the EUROfusion Consortium and has received funding from the Euratom research and training programme 2014-2018 under grant agreement No 633053. The views and opinions expressed herein do not necessarily reflect those of the European Commission.

DIFFER is a part of the Netherlands Organisation for Scientific Research (NWO) and a partner in the Trilateral Euregio Cluster TEC.

References

[1] G. Pintsuk, 4.17 - Tungsten as a Plasma-Facing Material, in: R.J.M. Konings (Ed.) Comprehensive Nuclear Materials, Elsevier, Oxford, 2012, pp. 551-581.

[2] R.A. Pitts, S. Carpentier, F. Escourbiac, T. Hirai, V. Komarov, S. Lisgo, A.S. Kukushkin, A. Loarte, M. Merola, A. Sashala Naik, R. Mitteau, M. Sugihara, B. Bazylev, P.C. Stangeby, A full tungsten divertor for ITER: Physics issues and design status, J. Nucl. Mater., 438, Supplement (2013) S48-S56.

[3] H. Kurishita, H. Arakawa, S. Matsuo, T. Sakamoto, S. Kobayashi, K. Nakai, G. Pintsuk, J. Linke, S. Tsurekawa, V. Yardley, K. Tokunaga, T. Takida, M. Katoh, A. Ikegaya, Y. Ueda, M. Kawai, N. Yoshida, Development of Nanostructured Tungsten Based Materials Resistant to Recrystallization and/or Radiation Induced Embrittlement, Mater. Trans., 54 (2013) 456-465.

[4] H. Kurishita, S. Matsuo, H. Arakawa, T. Sakamoto, S. Kobayashi, K. Nakai, H. Okano, H. Watanabe, N. Yoshida, Y. Torikai, Y. Hatano, T. Takida, M. Kato, A. Ikegaya, Y. Ueda, M. Hatakeyama, T. Shikama, Current status of nanostructured tungsten-based materials development, Phys. Scr., T159 (2014) 014032.

[5] M. Oya, K. Uekita, H.T. Lee, Y. Ohtsuka, Y. Ueda, H. Kurishita, A. Kreter, J.W. Coenen, V. Philipps, S. Brezinsek, A. Litnovsky, K. Sugiyama, Y. Torikai, Deuterium retention in Toughened, Fine-Grained Recrystallized Tungsten, J. Nucl. Mater., 438, Supplement (2013) S1052-S1054.

[6] M. Oya, H.T. Lee, Y. Ohtsuka, Y. Ueda, H. Kurishita, M. Oyaidzu, T. Yamanishi, Deuterium retention in various toughened, fine-grained recrystallized tungsten materials under different irradiation conditions, Phys. Scr., T159 (2014) 014048.

[7] M. Zibrov, M. Mayer, E. Markina, K. Sugiyama, M. Betzenbichler, H. Kurishita, Y. Gasparyan, O.V. Ogorodnikova, A. Manhard, A. Pisarev, Deuterium retention in TiC and TaC doped tungsten under low-energy ion irradiation, Phys. Scr., T159 (2014) 014050.

[8] M. Oya, H.T. Lee, Y. Ueda, H. Kurishita, M. Oyaidzu, T. Hayashi, N. Yoshida, T.W. Morgan, G. De Temmerman, Surface morphology changes and deuterium retention in Toughened, Fine-grained Recrystallized Tungsten under high-flux irradiation conditions, J. Nucl. Mater., 463 (2015) 1037-1040.

[9] M. Zibrov, M. Mayer, L. Gao, S. Elgeti, H. Kurishita, Y. Gasparyan, A. Pisarev, Deuterium retention in TiC and TaC doped tungsten at high temperatures, J. Nucl. Mater., 463 (2015) 1045-1048.
[10] A. Manhard, M. Balden, S. Elgeti, Quantitative Microstructure and Defect Density Analysis of Polycrystalline Tungsten Reference Samples after Different Heat Treatments, Practical Metallography, 52 (2015) 437-466.
[11] G.J. van Rooij, V.P. Veremiyenko, W.J. Goedheer, B. de Groot, A.W. Kleyn, P.H.M. Smeets, T.W. Versloot, D.G. Whyte, R. Engeln, D.C. Schram, N.J.L. Cardozo, Extreme hydrogen plasma densities achieved in a linear plasma generator, Appl. Phys. Lett., 90 (2007) 121501.
[12] G. De Temmerman, J.J. Zielinski, S. van Diepen, L. Marot, M. Price, ELM simulation experiments on Pilot-PSI using simultaneous high flux plasma and transient heat/particle source, Nucl. Fusion, 51 (2011) 073008.
[13] R.A. Felice, The Spectropyrometer—a Practical Multi-wavelength Pyrometer, AIP Conference Proceedings, 684 (2003) 711-716.
[14] G. Pintsuk, H. Kurishita, J. Linke, H. Arakawa, S. Matsuo, T. Sakamoto, S. Kobayashi, K. Nakai, Thermal shock response of fine- and ultra-fine-grained tungsten-based materials, Phys. Scr., T145 (2011) 014060.
[15] M. Mayer, E. Gauthier, K. Sugiyama, U. von Toussaint, Quantitative depth profiling of deuterium up to very large depths, Nucl. Instr. Meth. B, 267 (2009) 506-512.
[16] K. Schmid, U. von Toussaint, Statistically sound evaluation of trace element depth profiles by ion beam analysis, Nucl. Instr. Meth. B, 281 (2012) 64-71.
[17] M. Mayer, SIMNRA User's Guide, Report IPP 9/113, Max-Planck-Institut für Plasmaphysik, Garching, Germany, 1997.
[18] E. Salançon, T. Dürbeck, T. Schwarz-Selinger, F. Genoese, W. Jacob, Redeposition of amorphous hydrogenated carbon films during thermal decomposition, J. Nucl. Mater., 376 (2008) 160-168.
[19] P. Wang, W. Jacob, L. Gao, T. Dürbeck, T. Schwarz-Selinger, Comparing deuterium retention in tungsten films measured by temperature programmed desorption and nuclear reaction analysis, Nucl. Instr. Meth. B, 300 (2013) 54-61.

[20] Relative Sensitivity Measurements of Gases, Gas Analysis Application Note 282, Hiden Analytical Ltd.
[21] K.A. Moshkunov, K. Schmid, M. Mayer, V.A. Kurnaev, Y.M. Gasparyan, Air exposure and sample storage time influence on hydrogen release from tungsten, J. Nucl. Mater., 404 (2010) 174-177.
[22] L. Gao, U. von Toussaint, W. Jacob, M. Balden, A. Manhard, Suppression of hydrogen-induced blistering of tungsten by pre-irradiation at low temperature, Nucl. Fusion, 54 (2014) 122003.
[23] M.H.J. 't Hoen, M. Balden, A. Manhard, M. Mayer, S. Elgeti, A.W. Kleyn, P.A. Zeijlmans van Emmichoven, Surface morphology and deuterium retention of tungsten after low- and high-flux deuterium plasma exposure, Nucl. Fusion, 54 (2014) 083014.
[24] M. Zibrov, M. Balden, T.W. Morgan, M. Mayer, Deuterium trapping and surface modification of polycrystalline tungsten exposed to a high-flux plasma at high fluences, Nucl. Fusion, 57 (2017) 046004.
[25] D. Di Stefano, R. Nazarov, T. Hickel, J. Neugebauer, M. Mrovec, C. Elsässer, First-principles investigation of hydrogen interaction with TiC precipitates in α-Fe, Physical Review B, 93 (2016) 184108.
[26] H.O. Pierson, Handbook of Refractory Carbides and Nitrides, William Andrew Publishing, Westwood, NJ, 1996.
[27] H. Ding, X. Fan, C. Li, X. Liu, D. Jiang, C. Wang, First-principles study of hydrogen storage in non-stoichiometric TiCx, J. Alloys Compd., 551 (2013) 67-71.
[28] S. Ryabtsev, Y. Gasparyan, M. Zibrov, A. Shubina, A. Pisarev, Deuterium thermal desorption from vacancy clusters in tungsten, Nucl. Instr. Meth. B, 382 (2016) 101-104.
[29] M. Zibrov, S. Ryabtsev, Y. Gasparyan, A. Pisarev, Experimental determination of the deuterium binding energy with vacancies in tungsten, J. Nucl. Mater., 477 (2016) 292-297.
[30] W. Möller, J. Roth, Implantation, Retention and Release of Hydrogen Isotopes in Solids, in: D.E. Post, R. Behrisch (Eds.) Physics of Plasma-Wall Interactions in Controlled Fusion, Springer US, Boston, MA, 1986, pp. 439-494.
[31] S.M. Myers, P.M. Richards, W.R. Wampler, F. Besenbacher, Ion-beam studies of hydrogen-metal interactions, J. Nucl. Mater., 165 (1989) 9-64.

[32] O.V. Ogorodnikova, Fundamental aspects of deuterium retention in tungsten at high flux plasma exposure, J. Appl. Phys., 118 (2015) 074902.
[33] K. Sato, S. Yamaguchi, M. Hirabayashi, Deuterium retention in TiC crystals prepared by zone melting method, J. Nucl. Mater., 133–134 (1985) 714-717.
[34] S. Nagata, S. Yamaguchi, H. Naramoto, Y. Kazumata, Lattice location of deuterium implanted in TiC, Nucl. Instr. Meth. B, 48 (1990) 231-234.
[35] M. Mayer, M. Balden, R. Behrisch, Deuterium retention in carbides and doped graphites, J. Nucl. Mater., 252 (1998) 55-62.
[36] T. Nozaki, H. Homma, Y. Hatano, Pressure-Composition Isotherms of TiC-H System at Elevated Temperatures, Mater. Trans., 52 (2011) 526-530.
[37] L. Buzi, G. De Temmerman, B. Unterberg, M. Reinhart, T. Dittmar, D. Matveev, C. Linsmeier, U. Breuer, A. Kreter, G. Van Oost, Influence of tungsten microstructure and ion flux on deuterium plasma-induced surface modifications and deuterium retention, J. Nucl. Mater., 463 (2015) 320-324.